IEEE Access
Multidisciplinary | Rapid Review | Open Access Journal

Received January 25, 2019, accepted February 22, 2019, date of publication March 4, 2019, date of current version March 25, 2019.

Digital Object Identifier 10.1109/ACCESS.2019.2902730

Assessment of Orchid Surfaces Using Top-Down Contact Angle Mapping

CÉSAR JANECZKO[1,2], CICERO MARTELLI[1,2], JOHN CANNING[1,3,4], AND GUILHERME DUTRA[1]

[1]Graduate Program in Electrical and Computer Engineering, Federal University of Technology-Paraná, Curitiba 80230-901, Brazil
[2]Department of Electronics, Federal University of Technology-Paraná, Curitiba 80230-901, Brazil
[3]*i*nterdisciplinary Photonics Laboratories, GBDTC, School of Electrical and Data Engineering, University of Technology Sydney, Sydney, NSW 2007, Australia
[4]Australian Sensing and Identification Systems, Sydney, NSW 2000, Australia

Corresponding author: César Janeczko (janeczko@utfpr.edu.br)

This work was supported in part by the Coordenação de Aperfeiçoamento de Pessoal de Nível Superior–Brasil (CAPES)–Finance Code 001.

ABSTRACT Top-down contact angle (CA) measurements are used to characterize the green leaves and purple flowers of both old and young the Cattleya warneri orchids. The top-down CA allows the characterization of large surfaces away from the leaf edge, avoiding traditional cutting required for side view CA measurement. This allows large area mapping without damaging leaves making the method amenable to fieldwork and useful in environmental diagnostics. Young leaves are found to be hydrophobic whilst old leaves become practically hydrophilic across their entirety, mostly as a result of continued exposure to changes in the environment over time. The flowers are hydrophobic because of their visual and tactile attractor function for pollinating animals and the self-cleaning of dirt and pathogens. Real-time measurement and mapping of CA of surfaces open a new tool to assess the long-term impact of plant aging, pollution, and more of organisms in the field. The method has clear applications elsewhere such as in industrial probing of surfaces and products.

INDEX TERMS Contact angle measurement technique, environmental monitoring, image analysis, lighting.

I. INTRODUCTION

The wettability differences of leaf and flower surfaces obtained by measuring the contact angle (CA) of a drop on these surface is used to classify the plant's leaves as shown in Figure 1 [2]. There is a clearly observed relationship between the wettability and the microstructure of the biological surfaces, their specific biological function and plant health. All these measurements, however, are done at the edges of leaves using conventional methods based on direct CA measurements when imaged from the side. These side-view measurements, limited close to the leaf edge by the imaging lens focal length, are inferred to be widely representative of the plant leaf surface. In this work, we used top-down CA measurements to map the wettability over the entire leaf, providing much greater representative information of the surface than has been possible to date.

The wetting of leaves and flowers provides substantive insight into the physiological condition of a plant. According to [3], chemical and physical (structural) surface properties of leaves and their behavior with the wettability have ecological significance. They are tied to process properties such as the rate of photosynthesis, degree of pathogen infection and the surrounding environmental quality. Others report the colonization of epiphytic microorganisms, such as filamentous fungi, yeasts, and bacteria [4], epidermal modifications for acid rain [5], all of which will impact the CA. For example, the wettability of leaves can be influenced by the amount of

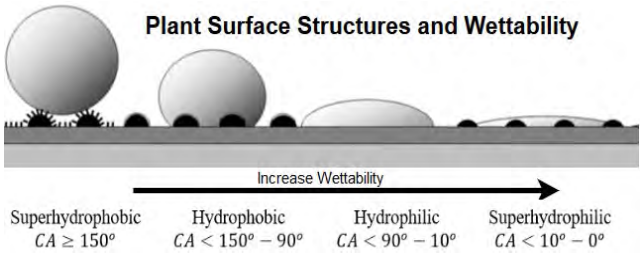

FIGURE 1. The four classes of surface wettability and characteristic static CA in a schematic demonstration of a possible surface sculpture of a plant. Adapted from [2].

The associate editor coordinating the review of this manuscript and approving it for publication was Irene Amerini.

FIGURE 2. Image of *Cattleya warneri*rubra "Werner Paske" orchid. The orchid is characterised by long green leaves and purple flowers.

air pollutants [6], particularly when trees that are sensitive to pollution are examined [7]. This can provide an indication of air quality over time of an urban habitat and contributes with environmental monitoring means. However, comprehensive utilization of such forensic information is generally not available because of the uncertainty and limitations of conventional side view measurements of CA. The top-down method solves several of these problems.

Another important reason for studying and mapping the surface of plants is the great diversity of biological surface structures arising from functional adaptations to environmental conditions during the evolution of terrestrial plants over the last 400 million years. Highly functional and protective biological interfaces in plants arise from self-assembled organized microstructures, orderly surface roughness or correlated disorganization on the leaf surface. These biological structures may provide more than one function. For example can both reflect light and demonstrate either superhydrophobicity or superhydrophilicity [8]. Recent interest and newly developed innovative techniques and materials can stimulate biomimetic research and transfer ideas and concepts implemented in nature into technology [9]–[11].

In this work we explore the utilization of top-down contact angle mapping (CAM) to characterize *Cattleya warneri* orchid leaves and flower (a plant image is shown in Figure 2) to assess their properties across the leaf and flower surface against those reported in the literature using standard side angle measurements. We demonstrate the increased reliability and potential of top down CA mapping CAM currently not feasible with side measurements without destroying the leaves, highlighting the valuable non-destructive method of this approach given its potential to be used in the field.

A. CONTACT ANGLE MEASUREMENTS USING TOP-DOWN IMAGING

Normally, CA measurements are made directly using lateral side imaging, where the CA is extracted by measuring the tangent at the triple phase point between the solid, liquid, and air surfaces [9]. This method is commonly known as the "tangent method." Other methods using spheroidal segments have been described and are less often used [12], [13]. Many recent studies point out several considerations for the characterization of surfaces through CA measurements including surface temperature and pressure [14], [15], evaporation [16]–[18] and gravity [19]. Reference [20] points to several sources of errors and possible solutions in the measurement of contact angle. However, none of these can perform large area mapping of the surface without it being progressively destroyed so the same issues apply to all. Consequently, the majority of analyses are near the edge. For vegetable surfaces, this would influence the measurement arising from the loss of water when the material under analysis is cut.

In the top-down method proposed in [1], the approach exploits the small volume of a liquid drop typically used in CA measurement so that the surface tension exceeds the gravitational force and a geometrical spherical caplet is assured. This makes mathematical analysis of the CA straight forward and easy to implement both for side view and top view analysis. Generally, values between $V \sim 2\ \mu$L to $5\ \mu$L are consistent and in accordance with the new handbook for standardized measurement of plant functional traits worldwide [21]. This small volume prevents the deformation of the droplet due to gravity, which can distort the shape of the droplet and hence the contact angle. Lateral measurement is a serious impediment to surface mapping, since deposition can be positioned only in the focal range of a lens near the edge of the surface image. Yet, the plants surface at the edges are not always flat or sufficiently homogeneous for use in side imaging. Top-down imaging is potentially simpler and, notably, can allow the mapping and acquisition of the CA measurements from top to bottom. The geometric nature of the spherical drop makes it possible to extract the CA directly from the measurements of the drop diameter. Reference [1] describes in detail the top-down approach and compares the lateral measurement approaches at the triple phase point between solid, liquid and air surfaces, and by the spheroidal segment method. In this work, its potential for characterization and mapping of plants is demonstrated.

B. SURFACE MAPPING

With top-down imaging, it is possible to map the surface wettability of large areas. The CA data can be combined with optical images to obtain a sophisticated colored representation of the surface characteristics allowing, for the first time, a tool to identify anomalous data, including contaminants and other properties. The method is reliable, simple, and robust, comparable to lateral imaging methods, making them potentially more practicable and most importantly field-deployable. The potential of mapping very large areas quickly opens a new area of diagnosis, enabling mass diagnostics for botanical and biomedical applications, quality control for industrial applications, chemical analysis, forensic research studies and so on. The method can be readily automated with

FIGURE 3. Flowchart of the developed algorithm.

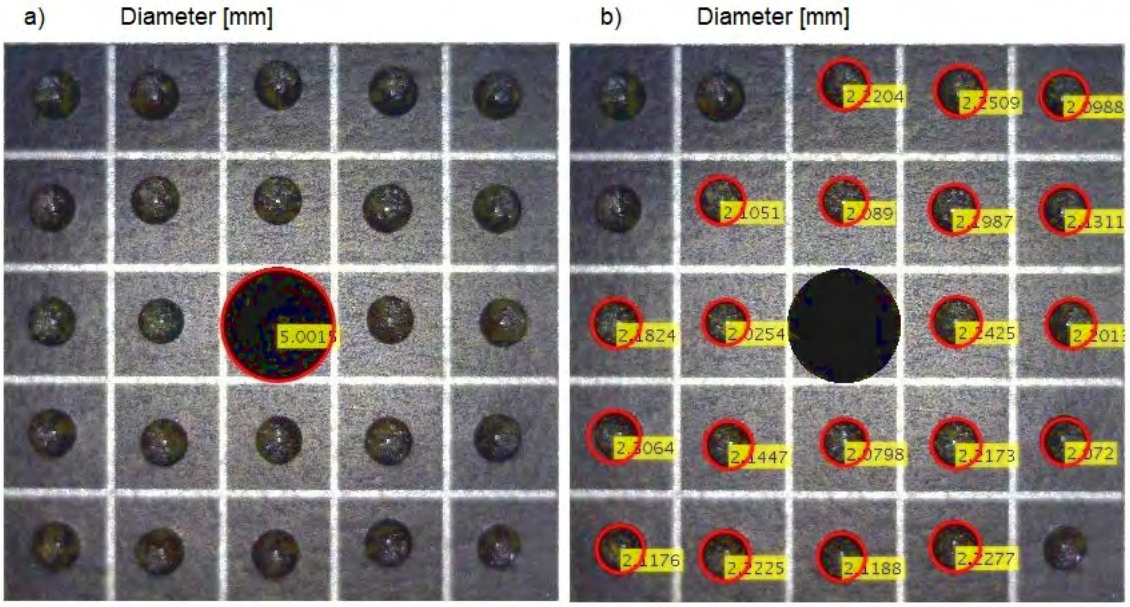

FIGURE 4. Method for calibrating the pattern recognition algorithm using laser printing on Aspen paper.

image pattern recognition software, working on a variety of mobile devices, including smartphones and tablets [1].

II. METHODOLOGY

Using top-down imaging, an image recognition algorithm was developed to measure the CA through the diameter and obtain a map of the surface wettability of the leaves and petals. Because of the difficulty in measuring the angle of contact, using conventional methods by the lateral view on plants surfaces that have imperfections, such as curvatures, roughness, and undesirable reflections, this automatism is impressive in facilitating the biological study of plants and animals. Figure 3 shows the flow diagram of the developed algorithms. More details on the algorithms are presented in the following sections.

A. IMAGE ACQUISITION AND PREPROCESSING

A micropipette (Labnet®, V = 2-20 μL; accuracy $\pm$ 5 %) is used to create the droplets that have the same volume ($V = 4\ \mu$L). For water this volume is small enough to ensure the surface tension is higher than the gravitational force, generating the spherical caplet required for the drops.

A portable mini-microscope (Dino-lite ^{TM}, magnification, 20$\times$ to 230$\times$) is connected to a computer to capture the top-down images of the drops. For the algorithm calibration, a matrix of squares $A = (5 \times 5)$ mm^2 is printed on Aspen paper and used as a reference for the deposition of the drops. In Figure 4, the acquired image receive manually in (a) a circle (diameter $\phi = 5$ mm) into the image editor is used to calibrate the algorithm. In this case, only the 5 mm circle was detected placing a restriction in finding the search range radii between $\phi = 4.5$ and 5.5 mm imposed by the developed algorithm; in (b), the search range radii was $\phi =$ (1.5 to 2.5) mm to detect the droplet diameters.

Finding suitable lighting to image the circle detection area for image processing was challenging due to the high reflectivity off the leaf wax which reduces contrast. The use of lighting rings for macrophotography and other powerful light sources with diffusers were impacted by this reflection. The solution to this illumination problem was to use two high-power white LEDs with convergent lenses at a distance of about 1 m vertically from the surface. Thereby, we have two almost punctual sources with near-parallel rays incident on the sample. This illumination reduces the size of the reflected spot seen in the drops.

Figure 5 shows the acquisition setup used is shown and a schamatic illustration is shown in Figure 6. Incident light (yellow rays) reflect off the sample towards the microscope lens (green rays) making these regions bright in the acquired image. Some of the illumination that reaches the droplets is reflected out of the acquisition field of the microscope (red rays). The contrast makes the droplets darker than the background and is used to detect and define the circular droplet area using software. The leaves and petals generally

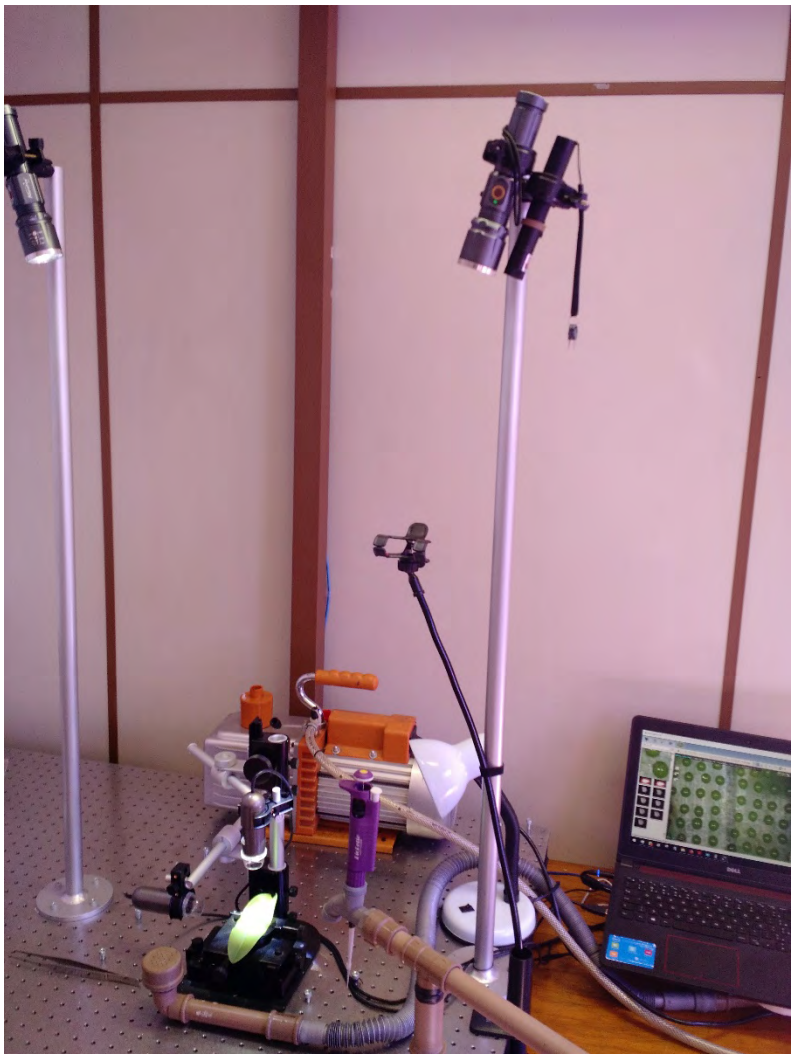

FIGURE 5. Image of acquisition system setup. A green leaf can be seen illuminated by the directed lights from above.

have curvatures that interfere in the deposition of the drops and consequently in the quality of the image. To solve this, we developed a polymeric substrate surface with small holes to suck the samples through a vacuum pump to improve the flatness of the sample. The negative pressure and the time are insufficient to damage the sample either mechanically or through drying. This flatness decreases the dark regions caused by curvature that reflects incident rays going out of the field of acquisition of the microscope lens.

To better understand the illumination, direct reflection from the sample and from the drop deposited on the sample were numerically simulated using a ray tracing method (Figure 7). In the coordinate $x,y = (0, 0)$ the light source is positioned and yellow rays go out to the sample 100 cm from the source. Green rays represent the incident rays that are reflected from the sample. In position $x,y = (25,100)$, a drop with $\varphi = 4$ mm is placed on the surface of the sample. By analyzing the simulation results it is possible to optimize the contrast between the bright background and dark drop images acquired by the microscope. Also, the brighter point observed in the drops in Figure 8 is a result of lensing from the circular droplet. This simulation does not consider the effect of secondary iterations such as reflections on the drops and diffusion of the rays due to imperfections and surface structures. Also, only a light source on the left side is considered and not the two light sources. The colors of the rays are the same as that used in Figure 6.

B. ALGORITHM FOR IMAGING PROCESSING

There are several algorithms for finding circles in images in the literature [22] and [23]. In this work an algorithm that is a variation of the classic algorithm based on Circular Hough Transform (CHT) is used following that described in [24]. It is noise tolerant and is sensitive to a range in the rays. CHT is not a strictly specified algorithm, and there are several different approaches that can be taken in its implementation. However, in general, there are three essential steps common to all:

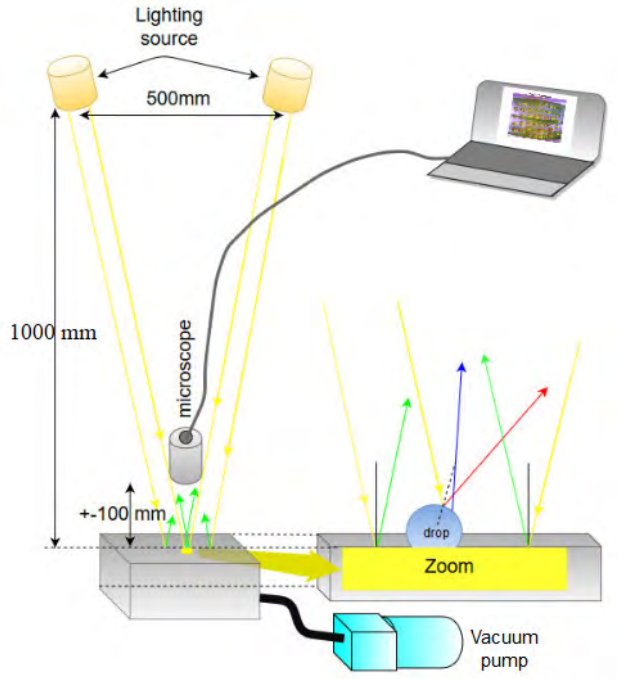

FIGURE 6. Schematic representation of the image acquisition system.

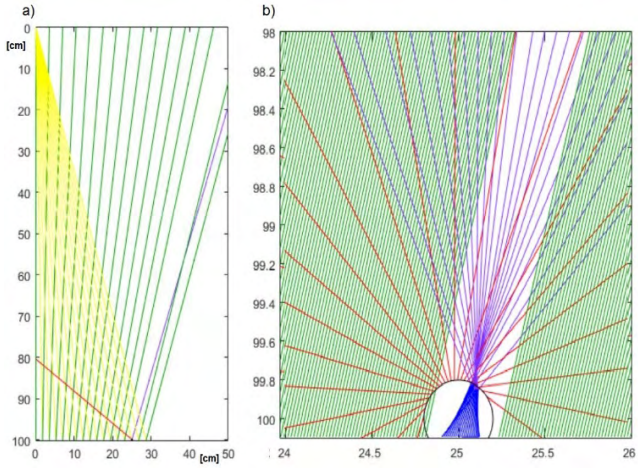

FIGURE 7. (a) Ray tracing simulation of illumination on leaf and drop surfaces. (b) Zoom.

1) Accumulator array computing: A process of choosing circles is used where votes or weights are assigned to the locus of possible circles in the image. The weights are summed in an accumulation array, and the circle detection is obtained when a maximum value (peak) is obtained [23].
2) Center estimation: The votes of the candidate pixels belonging to a real circle of the image tend to accumulate in the position corresponding to the center of the circle. Therefore, the centers of the circles are estimated by detecting the peaks in the accumulator array.
3) Radius estimation: If the same set of accumulators is used for radius values, as is usually done in CHT algorithms, the radii of the detected circles are estimated as a separate step.

The algorithm implemented in this work uses a 2-D array of accumulators. Although the classic CHT requires a 3-D array to store votes for multiple radius, resulting in large-storage requirements and long processing times, this is a widely adopted approach in modern CHT implementations because it reduces processing times and data generation [25]. Other features of the algorithm is the use of edge pixels to limit the number of candidate pixels and to define the magnitude of the input image gradient as the threshold, so that only the high gradient pixels are included in the counting votes. This works best when noise is low and contrast high.

The circle detector algorithm has as input the following information: the image, range of radii to be investigated,

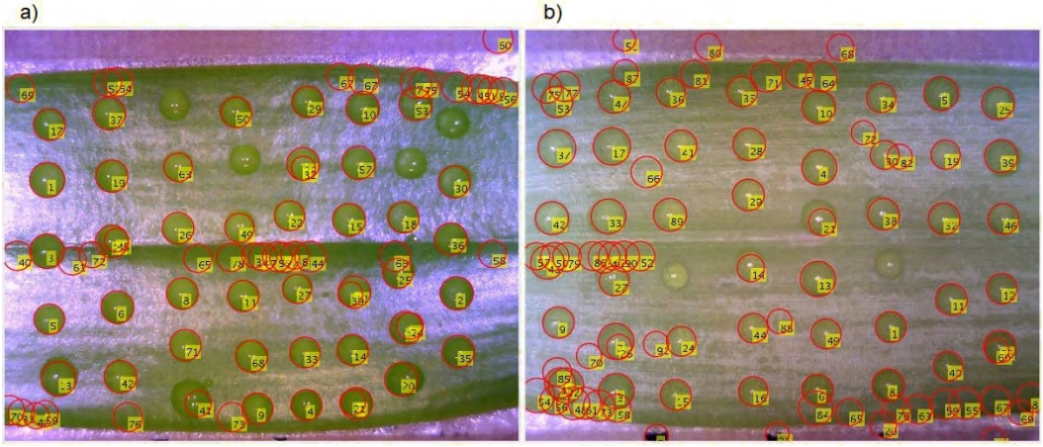

FIGURE 8. Detection order, in (a) the adaxial side (top) of the leaf of Cattleya walkeriana tipo, and in (b), the abaxial side (bottom).

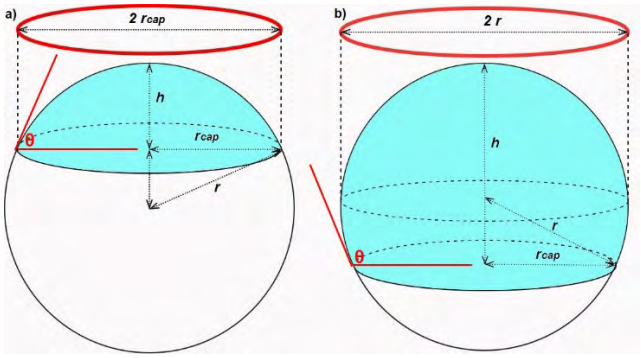

FIGURE 9. Schematic drawings to top-down imaging method for (a) omniphilic and (b) omniphobic surfaces.

the luminosity of the object (bright or dark), and the sensitivity, returning the center coordinates and the radius.

The sensitivity is a measure of the responsiveness to the accumulator array of the Circular Hough Transform. It is represented by a non-negative scalar value in the range of 0 to 1. As the sensitivity factor increases, the algorithm detects more circles, counting the partially obscured circles and weak circles. Hence, higher-sensitivity values also increase the risk of false positives or false detections.

Given the curvature of the plant surfaces, the image has many shadows, shown in Figure 8. These shadows can make drop detection difficult in these regions. To obtain the detection in these regions the sensitivity is increased but this may generate false positives. The performance of the proposed method is presented in Figure 8. The majority of the droplets deposited on the leaves surfaces are easily detected. However, ''false droplets'' or false positives are also detected. They can be reduced by changing the sensitivity value in algorithms input and adopting learning algorithms to refine the image analysis over time. In some cases, a visual inspection is also needed in order to guarantee that no false droplets are present. In table 1 the parameters employed in both calculations Figure 8 a) and Figure 8 b) are detailed. In more serious lighting situations, an alternative approach combined with vacuum assisted flattening of the sample, is to use polarizers to help reduce unwanted light reaching the microscope.

C. CONTACT ANGLE CALCULATION

A top view image of the spherical segment can lead to the two situations shown in Figure 9a, for omniphilic surfaces with CA $< 90°$ and Figure 9b, for omniphobic surfaces with CA $\geq 90°$.

When the algorithm returns the value of the radii of the circles detected, it is unknown if case (a) or case (b) is present. What is known is the radii of the circle seen from above and represented by the red circles in Figure 9. If the volume of the spherical caplet is $V_{cap} = \pi h/6 \cdot \left(3r_{cap}^2 + h^2\right)$ and that the CA is $\theta = 2atan\left(h/r_{cap}\right)$, then the CA is calculated using the flowchart shown in Figure 10.

D. SURFACE COLORFUL MAPPING

A major advantage of the top-down technique is the mapping of large surfaces. To facilitate visualization, surface mapping

TABLE 1. Input parameters used in the algorithm that generated Figure 8.

Sample	Butterworth mask	Cutoff frequency	Range Radii	Sensibility
7 a)	20x20	0.1	1.6 to 2.7	0.97
7 b)	-	-	1.6 to 2.7	0.9815

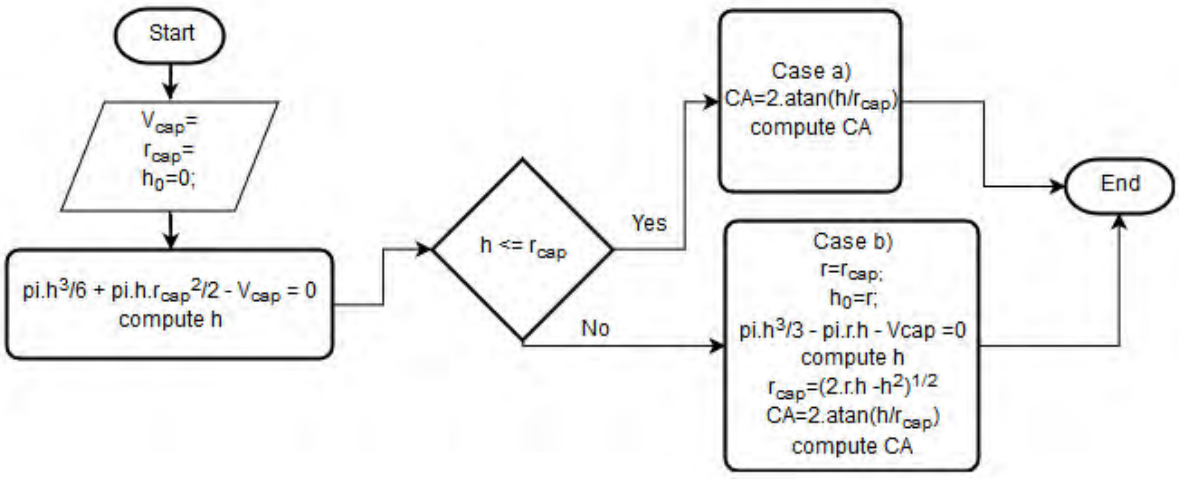

FIGURE 10. Flowchart to calculate CA (This flowchart presents a different form of CA calculation varying from the Top-down calculation method proposed by [1]).

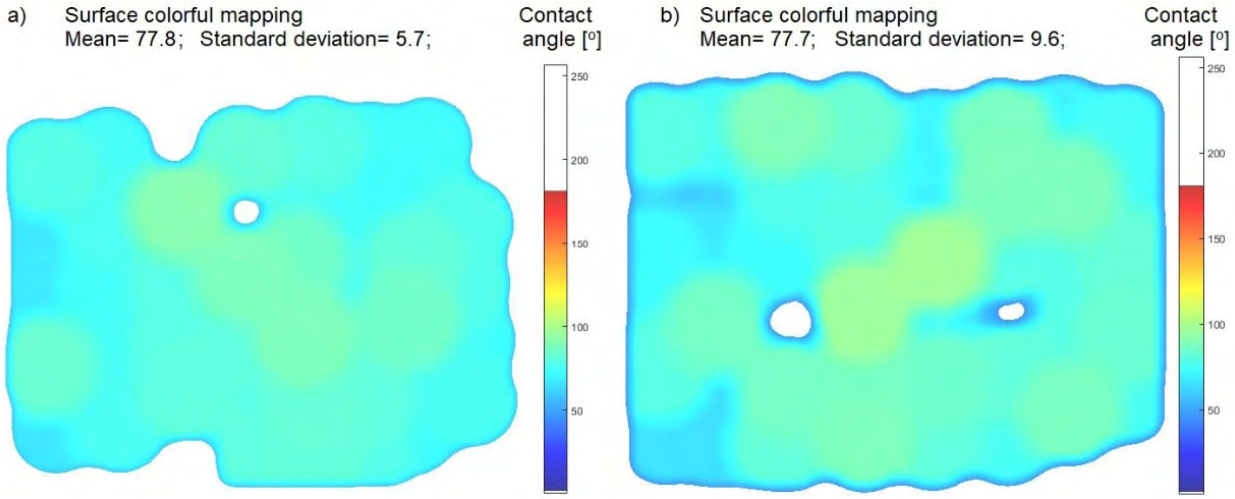

FIGURE 11. Surface color mapping according to the contact angle (values of CA = mean ± 3 × standard deviation).

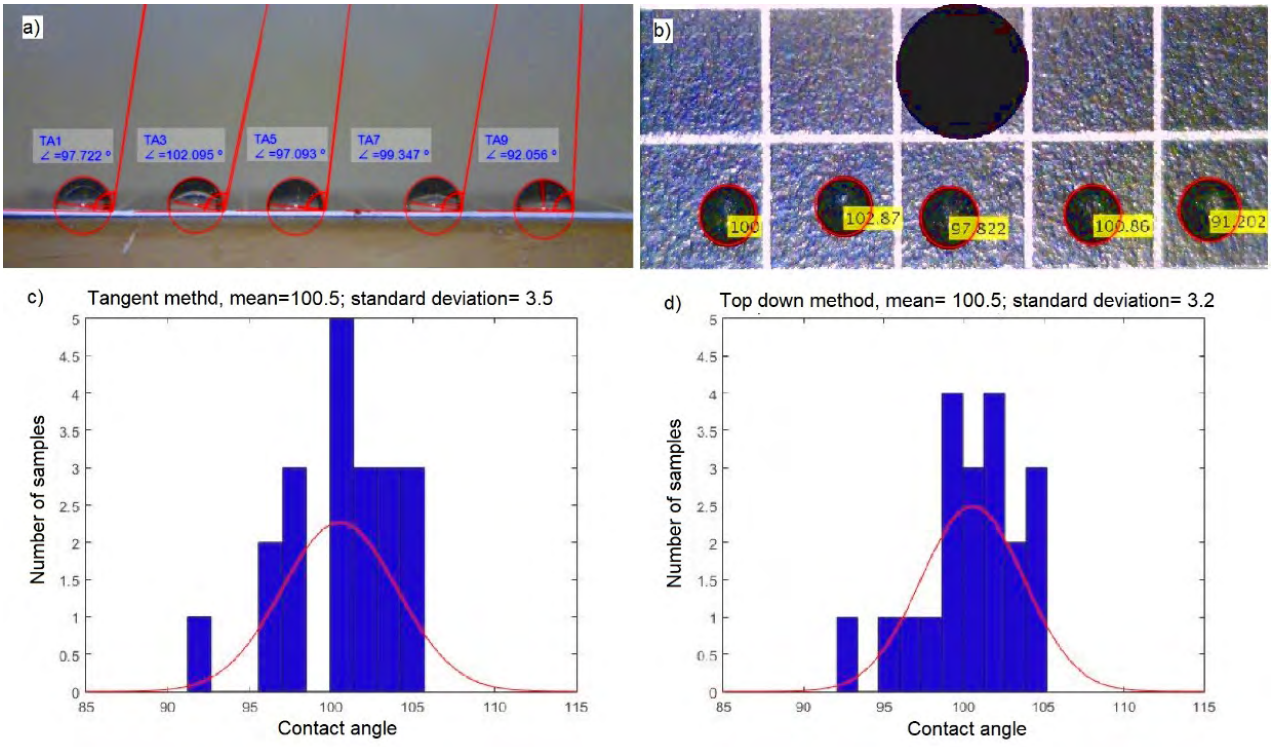

FIGURE 12. (a) Contact angles by the tangent method. (b) Contact angles by the top-down method. (c and d) Histograms, means, and standard deviations adjusted for the two methods respectively.

of the CA was undertaken in color. Given the regions with deposited drops are discontinuous in some places, an image morphological dilatation operation was used. In this case a structuring element in the form of a flat disk with origin in the center pixel and a radius specified according to the size and distance between the drops deposited on the surface is employed. The dilated image receives a third-order low-pass Butterworth filtration with cutoff frequency of 0.5 of the sampling frequencies with mask size of ± 70% of the disk diameter used as the dilation structuring element. This has the function of smoothing color transitions providing an ''interpolated'' representation of the surface. In Figure 11, an example, relating to the mapping of the detection shown in Figure 8.

E. VALIDATION

Validation of the method follows the work described in [1]. A print surface of an Aspen Brazilian paper sheet split into

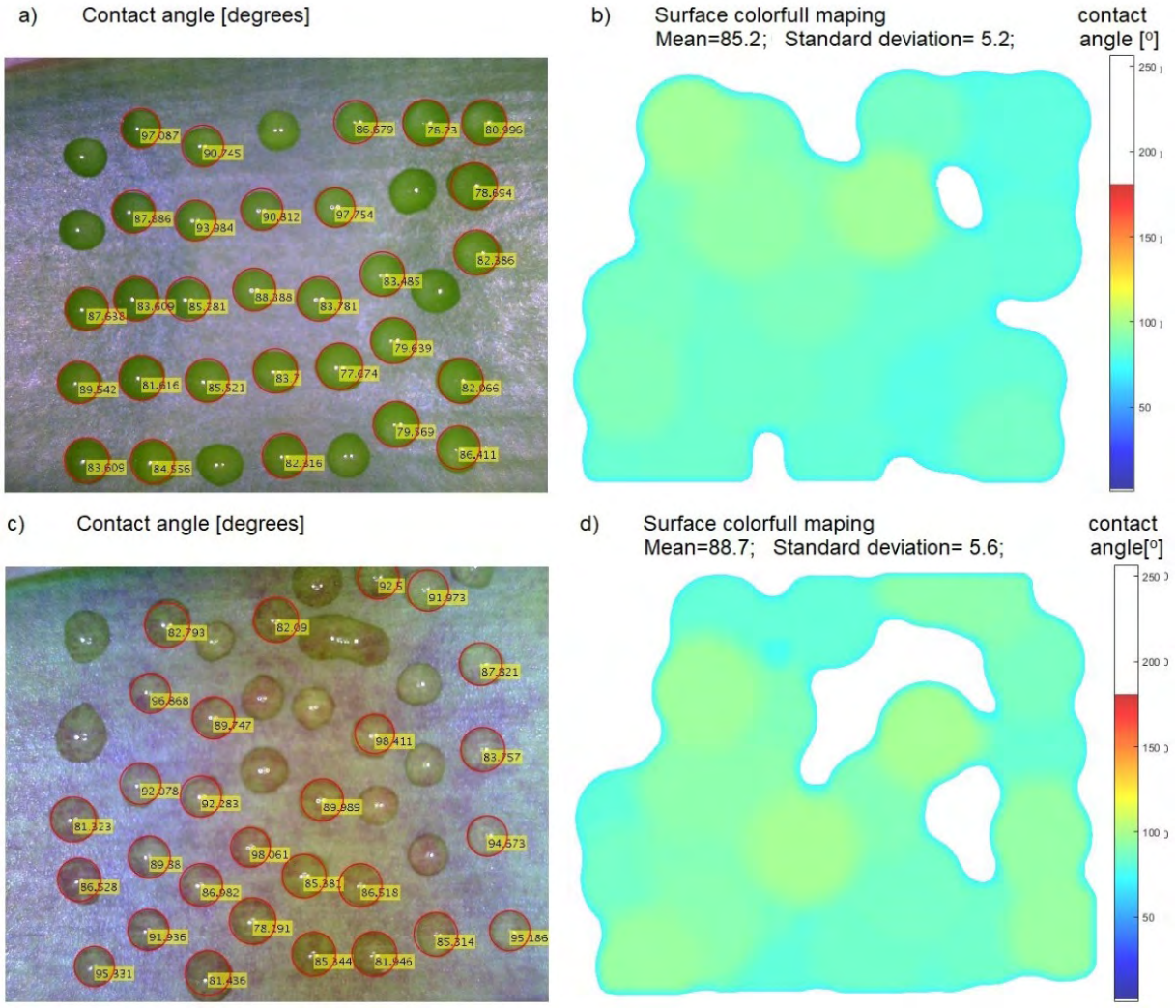

FIGURE 13. ***Cattleya warneri*** **rubra "Werner Paske" young leaf adaxial side (a), young leaf abaxial side (c). Mappings of the abovementioned surfaces (b and d), respectively.**

25 regions was used. The results are presented in Figure 12. Droplets of $V = 4\ \mu$ L were chosen to ensure no effect from gravity dependent shape changes at the water-air interface. Side view measurements were carried out as reference measurement method.

From Figure 12 the two CA measurement methods had similar and compatible results with errors in each arising from (Figure 12 a and c) manual positioning of the CA reference point and (Figure 12 b and d) issues described earlier such as the low-pass filter settings and the imperfect sensitivity factor used in the circle detection software as well as less than ideal illumination.

III. RESULTS AND DISCUSSION

The results of the CA evaluation of the adaxial and abaxial young and old leaves surface to *Cattleya warneri* rubra "Werner Paske" (Figure 13 and 14) and flowers surface to *Cattleya warneri* semi-alba (Figure 15) are presented and discussed.

Cattleya warneri rubra was chosen because of the intense pigmentation in the abaxial side of a young leaf (< 1 year old), due to sun exposure (figure 13c). The intense deposition of anthocyanins, in this case, is used by the plant for self-protection against UV radiation. In Figure 13 (a), the adaxial side to the same leaf is shown.

Figure 14 (a and b) belong to the adaxial and abaxial surfaces of the same plant. The leaf age is estimated to be $\sim$ 5 years because it is located on the same front and there are 5 posterior pseudobulbs (assuming the production of one pseudobulb occurs for each year).

The results observed in Figures 13 and 14 corroborates the existence of wettability change with leaf age, as expected according to [26] and [27]. In *Prickly Pear Cacti*, the young leaves are hydrophobic, and the old leaves are hydrophilic. This difference is because of the

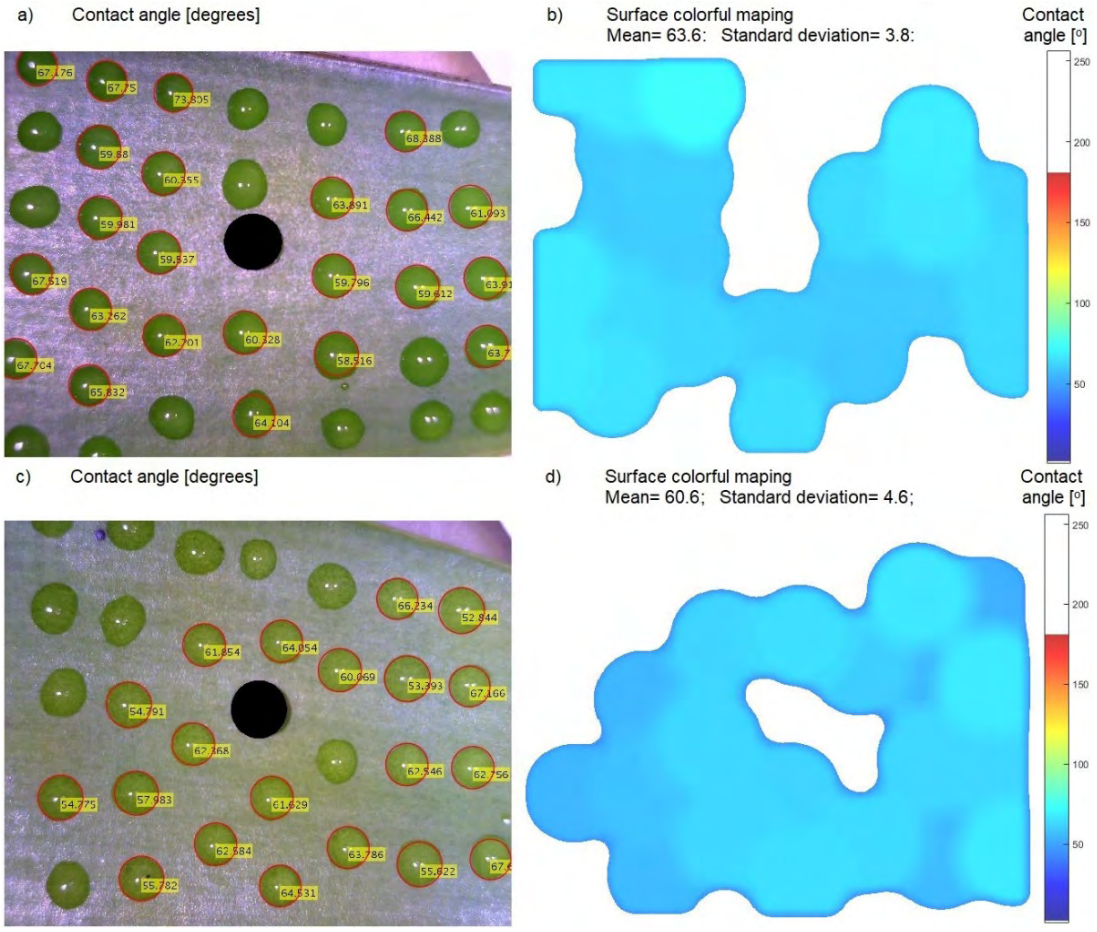

FIGURE 14. *Cattleya warneri* **rubra "Werner Paske" old leaf adaxial side (a), old leaf abaxial side (c). Mappings of the above mentioned surfaces (b and d), respectively.**

morphology change of the wax composition that was altered through a number of environmental stresses including solar incidence, wind, rainfall, and chemical exposure over the years. Since they vary drastically between different plants, the method can be used to monitor plant health over time [3].

Our measurements resulted in mean contact angles of $\theta = (85 \pm 15)°$ for the adaxial side of the young leaf and mean CA $\theta = (89 \pm 17)°$ for the abaxial side of the same leaf. For the 5 yr old leaf, the mean CA is $\theta = (64 \pm 11)°$ for the adaxial side and mean CA of $\theta = (61 \pm 14)°$ for the abaxial side. This result for the young leaf, low hydrophilic, is just below the transition to hydrophobic character, with a high contact angle. For the older leaf with a lower contact angle, the surface is much more hydrophilic. This difference occurs because of the impurities deposited on the leaf with age and the alteration of foliar microstructures with exposure to physical-chemical agents over time [26].

As for the side of the leaf, abaxial or adaxial, no great changes in the CA were observed, although the visual appearance is very different for the upper side that is brighter and the lower side that is somewhat opaque. However, from the viewpoint of image processing, this appearance changes the input parameters of the circle detection software (Table 2), as observed in the parameters used to generate Figures 13 and 14. The processing of the abaxial side, didn't require a low-pass filter. On the other hand the adaxial side, filtering is used because of the brightness of the leaves. In Figure 14 (a and b), a black circle with known diameter is deployed to recalibrate the software magnification parameter. This calibration changes when the support arm of the digital microscope is displaced. As the recalibration circle has different color and reflection of droplet behavior, an image editing software is used to superimpose the image arising from recalibration.

We can observe, for example in Figure 14 (c), in the upper left side due to inhomogeneity of the surface of the leaves or problems in their deposition, the drops occasionally appear deformed, not having a circular appearance. The top down method can identify this type of problem and discard such drops in the mapping when the deviation is too large, given that they no longer meet the spherical caplet approximation well. It is worth noting that the side view method may mask the measurement depending on which side the drop is

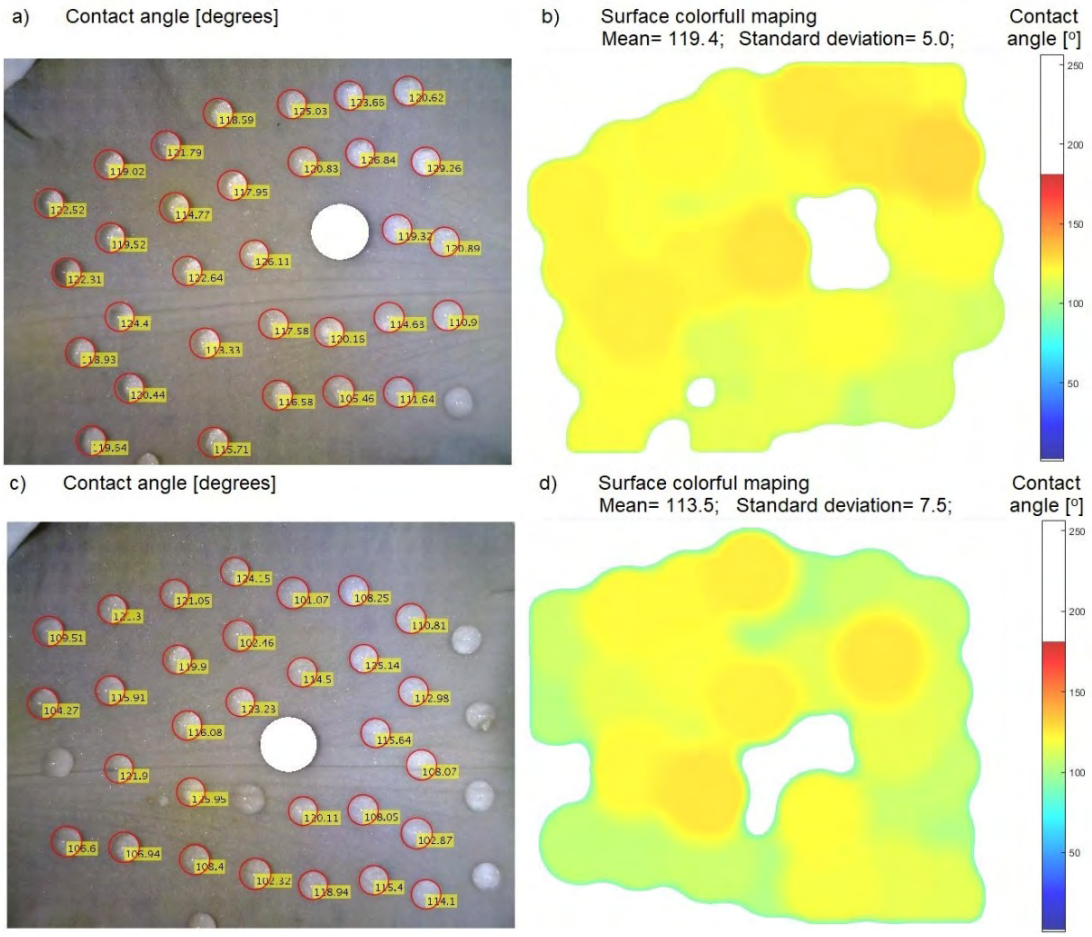

FIGURE 15. Flower of *Cattleya warneri* semi-alba (white petals and sepals with purple labellum), adaxial side (a) and abaxial side (c), in (b and d) the mapping of the cited surface respectively.

TABLE 2. Input parameters used in the algorithm that generated Figures 13 and 14.

Sample	Butterworth mask	Cutoff frequency	Range radii	Sensibility	Illumination
13a)	20×20	0.3	2.25 to 3.2	0.95	Dark
13 c)	-	-	2.3 to 3.2	0.989	Dark
14 a)	20 x 20	0.15	2.6 to 3.2	0.97	Dark
14 c)	-	-	2.6 to 3.3	0.985	Dark

TABLE 3. Input parameters used in the algorithm that generated Figure 15.

Sample	Butterworth mask	Cutoff frequency	Range radii	Sensibility	Illumination
15 a)	-	-	1.97 to 2.4	0.98	Bright
15 c)	-	-	1.9 to 2.4	0.985	Bright

examined. For plant leaves and insect wings, if drops are not axisymmetric, the contact angle depends on the direction of observation [20].

Figure 15, shows the CA surface mapping of the flower of the *Cattleya warneri* semi-alba for both the (a) adaxial side and abaxial side (c). The mean CA values were measured to be $\theta = (119 \pm 15)^\circ$ for the adaxial side of the flower and $\theta = (114 \pm 22)^\circ$ on the abaxial side; these have hydrophobic characteristics and are similar to each other and much larger than in the leaves. The result is consistent with [28] and [29] since the flowers have a visual and tactile attraction function for pollinating animals and can act to avoid wetting and optimize the self-cleaning of dirt and pathogens.

Table 3 presents the parameters used in the algorithm that generated Figure 15. The radii range is smaller than for the leaf surfaces. The change in detector algorithm input parameter to ''bright'' illumination is necessary because the drops are brighter than the background surface of the flower. This can

be accounted for by absorption or other resonant properties associated with the petal surface structures [30]. In contrast to the leaf measurements, where the drop is darker, in this case the magnification calibration circle used to recalibrate the circle detection software is a white circle.

IV. CONCLUSIONS

The results of novel top-down CA mapping measurements obtained in this leaf and flower wettability analysis of the orchid *Cattleya warneri* are in agreement and consistent with the theory found in the literature. Young leaves are hydrophobic, old leaves become practically hydrophilic mostly as a result of continued exposure to changes in the environment over time [26], [27]. These changes can include differences in air temperature, air relative humidity, soil moisture, frequency of precipitation events, and deposition of impurities. They modify the epicuticular waxes on the leaf surfaces altering the epidermal microstructures over time. The flowers are hydrophobic because of their visual and tactile attractor function for the pollinating animals, as well as the self-cleaning of dirt and pathogens [28], [29].

Based on the results obtained in this work, the automatic top-down method for measuring the CA and wettability mapping of biological surfaces is demonstrated, offering a powerful and rapid field-worthy approach and instrument for regular monitoring of plant health. To date, CA measurement has been a restricted scientific tool in the laboratory although it nonetheless provides a simple but powerful analysis of nanoscale interfaces of any type. Here, the method has been used to confirm and improve upon past work done on edge analysis with side measurements. The top down contact angle measurement can be applied more broadly and with greater certainty and confidence if only for the reason that the amount of measurements is greatly enhanced. This is further extended by statistical analysis. Further, the method described here can accommodate changes anywhere on a plant surface making it ideal for routine and ongoing diagnostics.

Moving away from difficult side imaging allows this nanoscale technique to reach into the field and to undertake scaled up numbers of measurements, potentially transforming research by enabling big data analysis across multiple internet-connected instruments measuring continually over time. An opportunity now exists for long term field studies to better understand plant health and aging in any environment over time, including the assessment of environmental and industrial pollutants introduced by word man into isolated environments. This is an exciting new area for environmentalists and botanists, as well as any expertise requiring much more rigorous forensic and scientific measure of environmental, industrial and organism impact than has been possible to date.

REFERENCES

[1] S. Dutra, G. Canning, J. Padden, W. Martelli, and C. Dligatch, "Large area optical mapping of surface contact angle," *Opt. Express*, vol. 25, no. 18, pp. 21127–21144, 2017.
[2] K. Koch, B. Bhushan, and W. Barthlott, "Diversity of structure, morphology and wetting of plant surfaces," *Soft Matter*, vol. 4, no. 10, pp. 1943–1963, 2008.
[3] H. Wang, H. Shi, and Y. Wang, *The Wetting of Leaf Surfaces and Its Ecological Significances*. London, U.K.: IntechOpen, 2015, pp. 295–321.
[4] D. Knoll and L. Schreiber, "Plant-microbe interactions: Wetting of Ivy (Hedera helix L.) leaf surfaces in relation to colonization by epiphytic microorganisms," *Microbial Ecol.*, vol. 40, no. 1, pp. 33–42, 2000.
[5] H. S. Neufeld, J. A. Jernstedt, and B. L. Haines, "Direct foliar effects of simulated acid rain," *New Phytol.*, vol. 99, pp. 389–405, Mar. 1985.
[6] J. Burkhardt, "Hygroscopic particles on leaves: Nutrients or desiccants?" *Ecol. Monogr.*, vol. 80, no. 3, pp. 369–399, 2010.
[7] F. Kardel, K. Wuyts, M. Babanezhad, T. Wuytack, S. Adriaenssens, and R. Samson, "Tree leaf wettability as passive bio-indicator of urban habitat quality," *Environ. Experim. Botany*, vol. 75, pp. 277–285, Jan. 2012.
[8] H. Bargel, K. Koch, Z. Cerman, and C. Neinhuis, "*Evans Review No. 3*: Structure–function relationships of the plant cuticle and cuticular waxes—A smart material?" *Funct. Plant Biol.*, vol. 33, no. 10, pp. 893–910, 2006.
[9] W. C. Bigelow, D. L. Pickett, and W. A. Zisman, "Oleophobic monolayers: I. Films adsorbed from solution in non-polar liquids," *J. Colloid Sci.*, vol. 1, no. 6, pp. 513–538, 1946.
[10] V. Fernández and M. Khayet, "Evaluation of the surface free energy of plant surfaces: Toward standardizing the procedure," *Frontiers Plant Sci.*, vol. 6, p. 510, Jul. 2015.
[11] P. Garg, P. Ghatmale, K. Tarwadi, and S. Chavan, "Influence of nanotechnology and the role of nanostructures in biomimetic studies and their potential applications," *Biomimetics*, vol. 2, no. 2, p. 7, 2017.
[12] J. Järnström, B. Granqvist, M. Järn, C.-M. Tåg, and J. B. Rosenholm, "Alternative methods to evaluate the surface energy components of ink-jet paper," *Colloids Surfaces A, Physicochem. Eng. Aspects*, vol. 294, nos. 1–3, pp. 46–55, 2007.
[13] G. L. Mack, "The determination of contact angles from measurements of the dimensions of small bubbles and drops. I. The spheroidal segment method for acute angles," *J. Phys. Chem.*, vol. 40, no. 2, pp. 159–167, 1935.
[14] F. Villa, M. Marengo, and J. De Coninck, "A new model to predict the influence of surface temperature on contact angle," *Sci. Rep.*, vol. 8, no. 1, 2018, Art. no. 6549.
[15] W. Wang and A. Gupta, "Investigation of the effect of temperature and pressure on wettability using modified pendant drop method," in *Proc. SPE Annu. Tech. Conf. Exhib.*, 1995, pp. 22–25.
[16] H. Y. Erbil, "Evaporation of pure liquid sessile and spherical suspended drops: A review," *Adv. Colloid Interface Sci.*, vol. 170, nos. 1–2, pp. 67–86, 2012.
[17] S. Semenov, A. Trybala, R. G. Rubio, N. Kovalchuk, V. Starov, and M. G. Velarde, "Simultaneous spreading and evaporation: Recent developments," *Adv. Colloid Interface Sci.*, vol. 206, pp. 382–398, Apr. 2014.
[18] H. Gelderblom *et al.*, "How water droplets evaporate on a superhydrophobic substrate," *Phys. Rev. E, Stat. Phys. Plasmas Fluids Relat. Interdiscip. Top.*, vol. 83, no. 2, 2011, Art. no. 026306.
[19] P. G. de Gennes, "Wetting: Statics and dynamics," *Rev. Mod. Phys.*, vol. 57, no. 3, p. 827, Jul. 1985.
[20] T. Huhtamäki, X. Tian, J. T. Korhonen, and R. H. A. Ras, "Surface-wetting characterization using contact-angle measurements," *Nature Protocols*, vol. 13, no. 7, pp. 1521–1538, 2018.
[21] N. Pérez-Harguindeguy *et al.*, "New handbook for standardised measurement of plant functional traits worldwide," *Austral. J. Botany*, vol. 61, no. 3, pp. 167–234, 2013.
[22] G. Duarte, "Uso da Transformada de Hough na Detecção de Círculos em Imagens Digitais," in *Thema-Revista Científica do Centro Federal de Educação Tecnológica do Rio Grande do Sul*. Pelotas, Brazil: Pelotas-RS-Brasil, 2003.
[23] R. O. Duda and R. E. Hart, "Use of the Hough transformation to detect lines and curves in pictures," *Commun. ACM*, vol. 15, no. 1, pp. 11–15, Jan. 1972.
[24] T. Atherton and D. J. Kerbyson, "Size invariant circle detection," *Image Vis. Comput.*, vol. 17, no. 11, pp. 795–803, Sep. 1999.
[25] T.-C. Chen and K. L. Chung, "An efficient randomized algorithm for detecting circles," *Comput. Vis. Image Understand.*, vol. 83, no. 2, pp. 172–191, 2001.
[26] K. Rykaczewski *et al.*, "Microscale mechanism of age dependent wetting properties of prickly pear cacti (*Opuntia*)," *Langmuir*, vol. 32, no. 36, pp. 9335–9341, 2016.

[27] V. Fernández *et al.*, "Wettability, polarity, and water absorption of holm oak leaves: Effect of leaf side and age," *Plant Physiol.*, vol. 166, no. 1, pp. 168–180, 2014.
[28] H. M. Whitney, R. Poetes, U. Steiner, L. Chittka, and B. J. Glover, "Determining the contribution of epidermal cell shape to petal wettability using isogenic antirrhinum lines," *PLoS ONE*, vol. 6, no. 3, 2011, Art. no. e17576.
[29] H. Taneda, A. Watanabe-Taneda, R. Chhetry, and H. Ikeda, "A theoretical approach to the relationship between wettability and surface microstructures of epidermal cells and structured cuticles of flower petals," *Ann. Botany*, vol. 115, no. 6, pp. 923–937, 2015.
[30] S. Vignolini, E. Moyroud, B. J. Glover, and U. Steiner, "Analysing photonic structures in plants," *J. Roy. Soc. Interface*, vol. 10, no. 87, 2013, Art. no. 20130394.

CÉSAR JANECZKO received the bachelor's degree in industrial electrical electronic engineering and the master's degree in industrial informatics with emphasis in biomedical engineering from the Federal University of Technology-Paraná, Curitiba, Brazil, in 1998 and 2000, respectively, where he is currently pursuing the Ph.D. degree in electrical and computer engineering-emphasis on biomedical engineering, researching the use of optics in the analysis of orchid leaves and flowers.

Since 1999, he has been a Lecturer with the Federal Technological University of Paraná. Since 2010, he has been a President of Auguste de Saint-Hilaire-Curitiba Botanical Garden Friend's Association. From 2011 to 2012, he was a Coordinator of the Superior Courses of Technology of the Academic Department of Electronics. From 2013 to 2014, he was the Head of the Academic Department of Electronics. He has experience in the area of biomedical engineering, with emphasis on digital processing of signals and images.

CICERO MARTELLI received the bachelor's degree in industrial electrical engineering and the master's degree in industrial informatics with an emphasis on opto-electronics from the Federal University of Technology-Paraná, Curitiba, Brazil, in 2002 and 2003, respectively, and the Ph.D. degree in engineering with the Interdisciplinary Photonics Laboratories/Optical Fiber Technology Center and the School of Electrical and Information Engineering, University of Sydney, in 2008.

He currently holds a professorial position with the Department of Electronics, Federal University of Technology-Paraná. He develops research projects on sensing systems, optical fibers, optical devices for communication, optical sensors, high power lasers, fiber optic lasers, laser light materials processing, non-linear optics, electro-optic coupling and molecular self-assembly.

JOHN CANNING is with the School of Electrical & Data Engineering at the University of Technology Sydney and runs the interdisciplinary Photonics Laboratories (iPL). He is an adjunct professor at the School of Electrical Engineering and Telecommunications, University of NSW, and Honorary Professor at the University of Sydney, and has cofounded several companies as well as helped to develop the technology of several others. He is a Fellow of SPIE and OSA. In 2017, he received the OSA David Richardson Medal for translating fundamental science to industry. He has been a Science Without Borders Professor (UTFPR 2015) in Brazil, a Program 1111 Professor (UESTC 2016) in China and has been Otto Monsted (DTU 2004) and Villum Kann Rasmussen Professor (Aarhus 2007) in Denmark. He has been an Expert Member of the University of Sydney's Latin Regional Advisory Committee and an Advisor to the China and India activities of the University. He has over 750 peer reviewed journal and conference papers and has lodged more than 35 patents.

GUILHERME DUTRA received the degree in industrial automation technology, the degree in production engineering in control and automation and the master's degree in electrical engineering and industrial informatics with emphasis in photonics from the Federal University of Technology-Paraná, Curitiba, Brazil, in 2009, 2011, and 2013, respectively, and the Ph.D. degree in electrical and computer engineering from UTFPR, in 2018.

His research interests include optical fibers, optical devices for communication, optical sensors, high power lasers, industrial automation, and electric machines.